

MetaSymNet: A Dynamic Symbolic Regression Network Capable of Evolving into Arbitrary Formulations

YanjieLi^{1,3}, WeijunLi^{1,2,3,*}, LinaYu¹ MinWu¹ JinyiLiu^{1,3} WenqiangLi^{1,2} MeilanHao¹ ShuWei^{1,2}
YusongDeng^{1,2}

¹ANMLAB, Institute of Semiconductors, Chinese Academy of Sciences, Beijing, China

²School of Electronic, Electrical and Communication Engineering, University of Chinese Academy of Sciences, Beijing, China

³School of Integrated Circuits, University of Chinese Academy of Sciences, Beijing, China
liyanjie21@ucas.edu.cn

Abstract

Mathematical formulas serve as the means of communication between humans and nature, encapsulating the operational laws governing natural phenomena. The concise formulation of these laws is a crucial objective in scientific research and an important challenge for artificial intelligence (AI). While traditional artificial neural networks (MLP) excel at data fitting, they often yield uninterpretable "black box" results that hinder our understanding of the relationship between variables x and predicted values y . Moreover, the fixed network architecture in MLP often gives rise to redundancy in both network structure and parameters. To address these issues, we propose MetaSymNet, a novel neural network that dynamically adjusts its structure in real time, allowing for both expansion and contraction. This adaptive network employs the PANGU meta-function as its activation function—a unique type capable of evolving into various basic functions during training to compose mathematical formulas tailored to specific needs. We then evolve the neural network into a concise, interpretable mathematical expression. To evaluate MetaSymNet's performance, we compare it with four state-of-the-art symbolic regression algorithms across more than 10 public datasets comprising 222 formulas. Our experimental results demonstrate that our algorithm outperforms others consistently regardless of noise presence or absence. Furthermore, we assess MetaSymNet against MLP and SVM regarding their fitting ability and extrapolation capability—two essential aspects in machine learning algorithms. The findings reveal that our algorithm excels in both areas. Finally, we compared MetaSymNet with MLP using iterative pruning in network structure complexity. The results show that MetaSymNet's network structure complexity is obviously less than MLP under the same goodness of fit.

Introduction

Finding a simple and clear interpretable mathematical expression from data is an important area of artificial intelligence research. In recent years, deep neural networks have been widely used in various fields of natural science (Liu et al. 2017; Abd Elaziz et al. 2021; Mamoshina et al. 2016). Although the traditional fully connected neural networks can fit the data very well, the traditional neural network structure is usually fixed, which is easy to cause redundancy of structure and parameters (Cheng et al. 2015). Moreover, the activation

function of ordinary fully connected neural networks is usually fixed, which affects the representation ability of neural networks to a certain extent. This forced the neural network to use more complex network structures in order to fit the curve better (Sun et al. 2016). Moreover, the result obtained by traditional neural network training is an uninterpretable "black box" (Afnan et al. 2021; Guidotti et al. 2018), which makes the results obtained by neural networks untrustworthy in many scenarios, especially in the medical field. (Yanco et al. 2016)

Therefore, in order to solve the above problems, we propose a novel tree-based neural network called MetaSymNet. The structure of the neural network is dynamically learnable and can be adjusted dynamically and adaptively according to the complexity of the task in real time. Moreover, we propose a new activation function named PANGU function, PANGU function can adaptively evolve into a variety of basic functions in the training process, which can greatly improve the problem of insufficient representation ability of ordinary neural networks. MetaSymNet is trained to produce a concise, interpretable mathematical expression (Narayanan et al. 2022; Marcinkevičs and Vogt 2020; Esterhuizen, Goldsmith, and Linic 2022). For example, consider a very classic formula in physics: $\mathcal{P} = \mathcal{F}\mathcal{V}$. From this formula, we can analyze that for a given power \mathcal{P} , if we want to get a larger force \mathcal{F} , we have to reduce the speed \mathcal{V} . This is also the theoretical guidance that we should reduce the speed when driving uphill in real life. However, when we take the force \mathcal{F} and the velocity \mathcal{V} as inputs to the neural network to predict the power \mathcal{P} . After training, the neural network can get a good fitting result such that $\mathcal{P} = f(\mathcal{F}, \mathcal{V})$, but from the black box function $f(\mathcal{F}, \mathcal{V})$, we can not analyze the relationship between the variables \mathcal{F} , \mathcal{V} and \mathcal{P} . In contrast, MetaSymNet can not only fit the power \mathcal{P} very well after training but also obtain the formula $\mathcal{P} = \mathcal{F}\mathcal{V}$ explicitly. Our contributions are summarized as follows:

- In this paper, a novel artificial neural network called MetaSymNet is proposed. The structure of MetaSymNet is not fixed but dynamically adjusted according to the complexity of the task. Moreover, the neuron type is not single but evolves into different types of neurons in real time according to the task requirements. The final result of network training is an interpretable mathematical expression.

Source code is provided at ¹.

- We propose a novel activation function, the PANGU meta-function, which can adaptively evolve into various other functions during the optimization process.
- We propose a method for neural networks to dynamically and adaptively adjust the network structure during training. This method can make the network structure become larger or smaller in real time under the guidance of gradient information.

Related Work

Based on Genetic algorithm The genetic algorithm (GA)(Mirjalili and Mirjalili 2019; Katoch, Chauhan, and Kumar 2021) is a classical algorithm that imitates human evolution, and the algorithm that applies the GA algorithm to solve the problem of symbolic regression is the Genetic Programming (GP) (Espejo, Ventura, and Herrera 2009; Fortin et al. 2012; Augusto and Barbosa 2000) algorithm. GP represents each expression in the form of a binary tree, initializes an expression population, and then evolves a better population by means of crossover, mutation, etc. Repeat the process until the termination condition is reached.

Based on reinforcement learning Deep Symbolic Regression (DSR)(Petersen et al. 2019) is a very good algorithm for symbolic regression using reinforcement learning. DSR uses a recurrent neural network as the strategy network of the algorithm, which takes as input the parent and sibling nodes to be generated, and outputs as the probability of selecting each symbol. DSR uses risk policy gradients to refine policy network parameters. DSO(Mundhenk et al. 2021) introduces the GP algorithm on the basis of DSR. This algorithm uses the formula sampled by DSR as the initial population of the GP algorithm and then performs crossover, mutation, and other operations through the GP algorithm to obtain a new population. Then DSO selects the n formulas with the highest reward function and mixes them with the data generated by DSR before, and finally updates the policy network RNN. Then DSR produces a better initial population for GP. Repeat the process. SPL(Sun et al. 2022) successfully applies MCTS to solve the problem of symbolic regression. In this algorithm, the author uses MCTS to explore the symbolic space and puts forward a modular concept to improve search efficiency.

Based on neural networks EQL(Martius and Lampert 2016; Kim et al. 2020) algorithm is a symbolic regression algorithm based on a neural network, which replaces the activation function in the fully connected neural network with basic operation symbols such as $[+, -, \dots, \sin, \dots]$, then optimizes the network through the backpropagation algorithm, and removes the excess connections through pruning, and then extracts an expression from the network. AI Feynman series algorithms are mainly divided into two versions, the main idea of this series of algorithms is to reduce complexity to simplicity. AI Feynman 1.0(Udrescu and Tegmark 2020) first uses a neural network to fit the data and then uses the curve fitted by the

neural network to analyze a series of properties in the data, such as symmetry and separability. Then the formula to be found is divided into simple units by these properties, and finally, the symbol of each unit is selected by random selection. The idea of AI Feynman 2.0(Udrescu et al. 2020) and 1.0 is very similar, the biggest difference between the two is that version 2.0 introduces more properties so that the search expression can be divided into simpler units, improving the search efficiency. Moreover, the application scenario of AI Feynman2.0 is no longer limited to the field of physics, and the application scope is more extensive.

Based on Transformer The NeSymReS(Biggio et al. 2021) algorithm treats the symbolic regression problem as a translation problem in which the input $[x, y]$, and the output is a preorder traversal of the expressions. NeSymReS first generates a number of expressions and then uses the sampled data $[x, y]$ from these expressions as inputs and the backbone of the expressions as outputs to train a transformer(Vaswani et al. 2017), pre-training model. When predicting the data, $[x, y]$ is entered into the transformer, and then combined with the beam search, a pre-order traversal of the formula is generated in turn. The biggest difference between the end-to-end algorithm and NeSymReS is that the end-to-end approach(Kamienny et al. 2022) can directly predict a constant to a specific value. Instead of predicting a constant placeholder "C".

Modeling

MetaSymNet is a tree-like neural network, in which each node can be regarded as a neuron, and the activation function of the node adopts the PANGU metafunction. In the process of training, in addition to optimizing amplitude parameters \mathcal{D} and bias term b like ordinary fully connected neural networks, we also optimize the internal Selecting parameters Z of the PANGU metafunction. After end-to-end training of the neural network, we not only fit the data very well, but also magically evolve the PANGU metafunction into various basic functions, and the network miraculously becomes an analyzable and interpretable mathematical formula. MetaSymNet's algorithm schematic is shown in Figure 1. See Appendix 1 for the pseudocode

We first randomly initialize a tree-like neural network with the number of neurons and the network structure arbitrarily given. The activation function of the neural network is the PANGU meta-function. In the beginning, each neuron has two inputs. Because our activation library contains not only unary activation functions like $[\sin, \cos, \exp, \sqrt{\cdot}, \log]$ but also binary activation functions like $[+, -, \times, \div]$, etc.

PANGU meta-function2

Normal neural network activation function is fixed, only the *relu* or *sigmoid* activation function, this leads to the neural network model being a bunch of combinations and nested activation functions and parameters, usually a complex and inexplicable "black box". To improve the above, we will extend the activation function of neural networks with several basic operators, such as $[+, -, \times, \div, \text{sincos}, \exp, \sqrt{\cdot}, \log, \dots]$. Because many formulas and theorems in natural science are

¹Source code for MetaSymNet: <https://anonymous.4open.science/r/MetSymNet-SR>

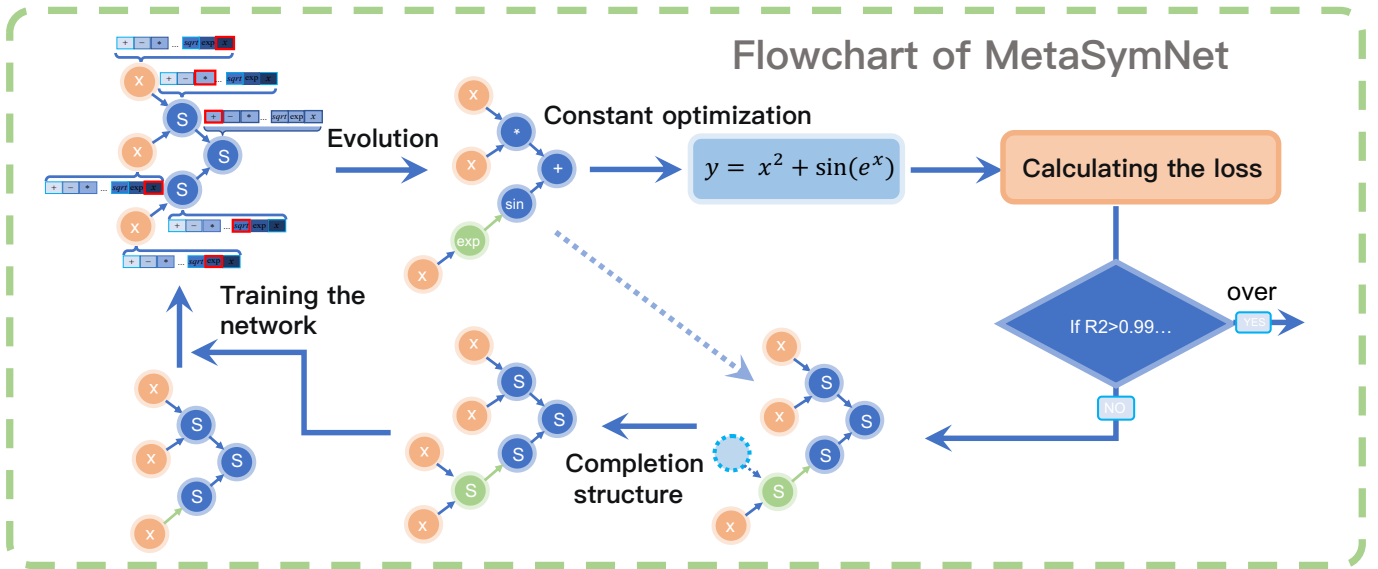


Figure 1: (i) First randomly initialize a network structure, where the internal node S is the PANGU meta-function and the leaf node x is the variable meta-function. (ii) Back propagation algorithm is used to optimize the parameters. In this process, the amplitude parameter \mathcal{D} and the bias parameter \mathcal{B} are optimized first, and then the internal parameters \mathcal{Z} and \mathcal{W} of the PANGU meta-function and variable meta-function are optimized. Iterate a number of times. (iii) After the parameter optimization, we choose the type of activation function that should be selected by leaf nodes and internal nodes and adjust the network structure at the same time. (iv) When the network evolves into an expression, we further optimize the parameters of the expression and calculate the loss and R^2 . The iteration stops when R^2 reaches the specified threshold. Otherwise, the iteration continues.

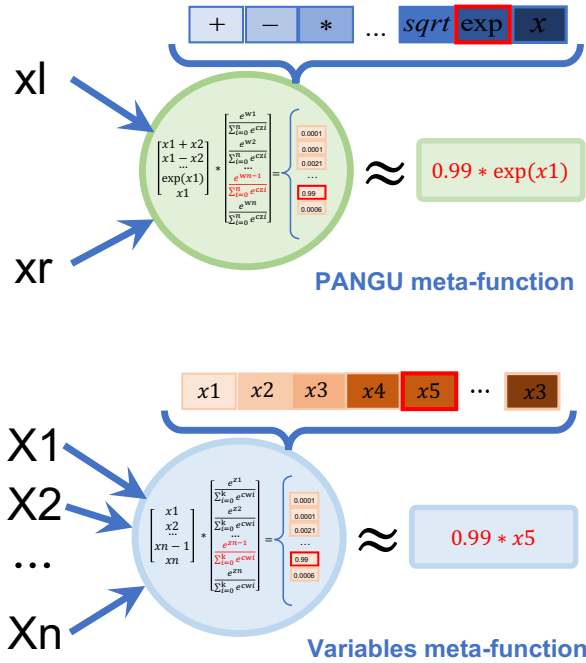


Figure 2: The figure depicts the detailed internal structure diagram of the PANGU metafunction (top) and variable metafunction (bottom).

composed of these basic operators. If the neural network is free to choose these activation functions, the resulting model will be a concise and interpretable mathematical formula. In order to realize the free choice of the activation function of the neural network, we design a PANGU meta-function. The formula is as follows 1:

$$OUT = d * [o_1, o_2, \dots, o_n] \begin{bmatrix} e_1 \\ e_2 \\ \dots \\ e_n \end{bmatrix} + b \quad (1)$$

Here, OUT is the corresponding output of the neural network, d , and b are parameters, and o_i is the output of the i^{th} activation function in the activation function library after numerical calculation of the neuron input. e_i is the probability of selecting each activation function in the activation function library, and the specific calculation formula of e_i can be reflected in Eq.2.

$$OUT = d * [x_l + x_r, \dots, \exp(x_l), x_1, \dots, x_n] \begin{bmatrix} \frac{e^{z_1}}{\sum_{i=1}^n e^{c * z_i}} \\ \frac{e^{z_2}}{\sum_{i=1}^n e^{c * z_i}} \\ \dots \\ \frac{e^{z_n}}{\sum_{i=1}^n e^{c * z_i}} \end{bmatrix} + b \quad (2)$$

Where $\mathcal{E} = softmax(\mathcal{Z} - max(\mathcal{Z}))$ (Stevens et al. 2021; Dong, Zhu, and Ma 2019), e_i is the i th value in vector \mathcal{E} , and $e_i = \frac{e^{z_i}}{\sum_{j=1}^n e^{c * z_j}}$. The vector $\mathcal{Z} = [z_1, z_2, \dots, z_n]$ is a set of selection parameters that can be optimized to control the probability of each activation function in the activation function library being selected. And all intra-neuron function

choice parameters \mathcal{Z} form the set $\mathbb{Z} = [\mathcal{Z}_1, \mathcal{Z}_2, \dots, \mathcal{Z}_n]$. Here n denotes the number of internal neurons.

Variables meta-function

At the leaf nodes of the network, we will initialize a variable selection meta-function, the principle of this function and PANGU meta-function is similar. And shown in Figure 2(bottom), but the function can only evolve into different variables $[x_1, x_2, \dots, x_n]$. Its expression is as follows 3:

$$OUT = d * [x_1, x_2, \dots, x_k] \left[\frac{e^{w_1}}{\sum_{i=1}^k e^{c * w_i}} \right] + b \quad (3)$$

Here is a set of variable selection parameters $\mathcal{W} = [w_1, w_2, \dots, w_k]$. Here, k is the number of variables in the task. And d is the amplitude control parameter and b is the bias parameter. In MetaSymNet, the variable selection parameter $\mathbb{W} = [\mathcal{W}_1, \mathcal{W}_2, \dots, \mathcal{W}_q]$ and the activation function selection parameter \mathbb{Z} are optimized simultaneously. Here, q denotes the total number of leaf nodes.

parameters optimization

Each neuron is assigned three types of parameters, an amplitude constant d , a bias constant b , and a set of selection parameters $\mathcal{Z} = [z_1, z_2, \dots, z_n]$. Here, the magnitude constants d of all neurons form the parameter set \mathcal{D} . Similarly, all bias constants b form the set \mathcal{B} , and all intra-neuron function choice parameters \mathcal{Z} form the set \mathbb{Z} . All variable selection parameters form the set \mathbb{W} . We alternately optimize the above types of parameters with a numerical optimization algorithm (For example, SGD(Bottou 2012, 2010), BFGS(Dai 2002), L-BFGS(Liu and Nocedal 1989) etc). First, the parameters in the set \mathcal{D} and \mathcal{B} are optimized for a certain number of times, and then the parameters in the set \mathbb{Z} and \mathbb{W} are optimized, and then the activation functions of each node and the variables of the leaf nodes are selected. Finally, after optimizing the parameters alternately for a number of rounds, we extract a formula from the network and further optimize \mathcal{D} and \mathcal{B} to achieve higher accuracy.

Activation function selection

There are many types of activation functions in the activation function library. This article contains four binary activation functions $[+, -, \times, \div]$, five unary activation functions $[\sin, \cos, \exp, \log, \text{sqrt}]$, and variables $[x_1, x_2, \dots, x_k]$. We initialize each neuron with an optimizable selecting parameter vector $\mathcal{Z} = [z_1, z_2, \dots, z_n]$, where n represents the class of functions to be selected from the activation library. We optimize \mathcal{Z} by backpropagation algorithm, Then the optimized \mathcal{Z}_{new} each element minus the $Max(\mathcal{Z}_{new})$, and then sent *softmax* classifier to get $\mathcal{E} = \text{softmax}(\mathcal{Z}_{new} - Max(\mathcal{Z}_{new})) = [e_1, e_2, \dots, e_n]$. For neuron \mathcal{S} , We assume that its two inputs are x_l and x_r , and then the functions in the activation functions library do the corresponding numerical operations respectively. We can obtain the vector $\mathcal{O} = [x_l + x_r, x_l - x_r, x_r * x_r, x_l/x_r, \sin(x_l), \cos(x_l), \exp(x_l), \log(x_l), \text{sqrt}(x_l), x_1, x_2, \dots, x_n]$. Finally, we dot multiply the vectors \mathcal{E} and \mathcal{O} , multiply by a constant d , and add a bias term b to get the output. After optimizing the vector \mathcal{Z} *Number* times in this way, we map \mathcal{Z} to one-hot(Rodríguez et al. 2018) form and then dot multiply it with \mathcal{O} . If the target expression is still not found, or R^2 is less than 0.9999. This process is repeated until a stopping condition is reached.

The variable metafunction selection process is as follows: First, we assume that the output of the optimized \mathcal{W} after passing through softmax is $\mathcal{O}_w, X * \mathcal{O}_w = v$. Then we select the two variables x_i, x_j with the largest probability according to \mathcal{O}_w as the input of this node. Then select the function corresponding to the value closest to v in vector $[x_i + x_j, x_i - x_j, \dots, \sin(x_i), \dots, x_1, \dots, x_n]$ as the activation function of the node

The variable metafunction selection process is as follows: First, we assume that the output of the optimized \mathcal{W} after passing through softmax is $\mathcal{O}_w, X * \mathcal{O}_w = v$. Then we select the two variables x_i, x_j with the largest probability according to \mathcal{O}_w as the input of this node. Then select the function corresponding to the value closest to v in vector $[x_i + x_j, x_i - x_j, \dots, \sin(x_i), \dots, x_1, \dots, x_n]$ as the activation function of the node

Loss function

In the process of neural network training, the loss function has a crucial position, because it directly determines the direction of neural network optimization. In this study, we introduce a new loss function that aims to further optimize the performance of neural networks. Our method covers the selection parameters \mathcal{Z} of each PANGU meta function, and these parameters are processed by softmax to obtain the vector $\mathcal{E} = [e_1, e_2, \dots, e_n]$. We introduce the entropy(Wehrl 1978; Rényi 1961) of \mathcal{E} as the loss function. Our goal is to make the largest element of the vector \mathcal{E} numerically significantly higher than other elements while maintaining the prediction accuracy of the model. Specifically, the expression for the loss function is as follows 4:

$$\mathcal{L} = \frac{1}{\mathcal{N}} \sum_{n=1}^{\mathcal{N}} (y_i - \hat{y}_i)^2 - \lambda \frac{1}{\mathcal{M}} \sum_{j=1}^{\mathcal{M}} \log(\max(\mathcal{E}_j)) \quad (4)$$

Where \mathcal{N} is the number of sample points, y is the true y value, and \hat{y} is the predicted y value. \mathcal{M} is the number of neurons under the current network structure, and \mathcal{E}_j is the value of the selection parameter of the j^{th} neuron after passing softmax. λ is the entropy loss regulation coefficient

Network Structure Optimization

The network structure of traditional neural networks is fixed, which is very easy to cause network structure redundancy. Although there are many pruning methods to simplify the structure of neural networks by pruning unnecessary connections, it is difficult to find a balance between the goodness of fit and the complexity of the network structure(Hermundstad et al. 2011; Maksimenko et al. 2018). We propose an algorithm to optimize the network structure in real time under the guidance of gradient. From the above, we can know that the activation function of our neural network can be learned dynamically. We designed a method to cleverly realize the dynamic adjustment of the network structure when the activation function changes. Specifically, in a neural network, each neuron has two inputs, and after training for a period of time, we determine the activation function of each neuron. The rules for adjusting the structure according to the activation function are as follows:

Dataset	Name	Number	MetaSymNet	DSO	EQL	GP	NeSymReS
Dataset-1	Nguyen	21	0.9999 ± 0.000	0.9999 ± 0.001	0.9544 ± 0.002	0.9186 ± 0.000	0.8468 ± 0.002
Dataset-2	Keijzer	15	0.9992 ± 0.001	0.9924 ± 0.001	0.9147 ± 0.002	0.8441 ± 0.001	0.7992 ± 0.002
Dataset-3	Korns	15	0.9999 ± 0.001	0.9872 ± 0.000	0.8271 ± 0.002	0.8139 ± 0.001	0.8011 ± 0.001
Dataset-4	Constant	8	0.9996 ± 0.002	0.9988 ± 0.003	0.8416 ± 0.001	0.8617 ± 0.003	0.8444 ± 0.002
Dataset-5	Livermore	22	0.9924 ± 0.003	0.9746 ± 0.003	0.7982 ± 0.002	0.8022 ± 0.003	0.7136 ± 0.0004
Dataset-6	Vladislavleva	8	0.9826 ± 0.003	0.9963 ± 0.004	0.8218 ± 0.004	0.7833 ± 0.003	0.6892 ± 0.004
Dataset-7	R	6	0.9921 ± 0.002	0.9744 ± 0.003	0.8628 ± 0.002	0.8772 ± 0.004	0.8003 ± 0.004
Dataset-8	Jin	6	0.9992 ± 0.0002	0.9916 ± 0.002	0.9221 ± 0.003	0.8872 ± 0.002	0.8627 ± 0.002
Dataset-9	Neat	9	0.9953 ± 0.0004	0.9827 ± 0.003	0.8633 ± 0.004	0.8127 ± 0.004	0.7996 ± 0.005
Dataset-10	AlFeynman	103	0.9940 ± 0.002	0.9610 ± 0.003	0.8722 ± 0.004	0.8827 ± 0.003	0.7025 ± 0.003
Dataset-11	Others	9	0.9992 ± 0.001	0.9861 ± 0.002	0.9247 ± 0.003	0.8763 ± 0.002	0.8226 ± 0.002
Average			0.9961 ± 0.003	0.9859 ± 0.008	0.8730 ± 0.03	0.8509 ± 0.03	0.7893 ± 0.04

Table 1: Comparison of the coefficient of determination (R^2) between MetaSymNet and four baseline. Bold values indicate state-of-the-art (SOTA) performance. The confidence level is 0.95

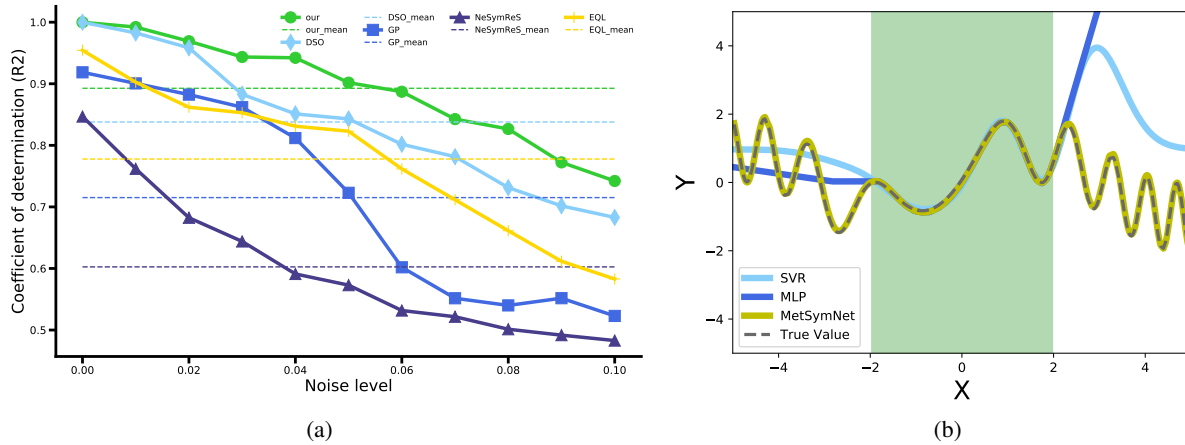


Figure 3: Figure (a) illustrates the trends of R^2 values between MetaSymNet and four baseline methods across varying noise levels. On the other hand, Figure (b) portrays the performance comparison of MetaSymNet, MLP, and SVR in terms of extrapolation ability. (Nguyen-6 : $\sin(x) + \sin(x + x^2)$).

- (1) when the PANGU meta-function evolves into a unary activation function, at this time, we replace the activation function of the node with a new activation function and only keep the first input of the neuron as the input of the new neuron. At this time, the number of network neurons will be reduced and the network structure will be simplified.
- (2) when the PANGU meta-function evolves into a binary activation function, at this time we replace the node activation function with a new activation function and keep all the two inputs. At this time, the network organization does not change.
- (3), when the PANGU metafunction evolves into the variable x_i , at which point we will discard all the inputs to the neuron. At this time, the number of neurons in the neural network becomes small, and the network structure is simplified.
- (4) When x_i evolves into a unary activation function, add a new neuron at x_i whose activation function is the newly selected unary activation function and takes the first variable selected as input. At this time, the growth of the network structure is realized.
- (5), when x_i evolves into a binary activation function, add a new neuron at x_i and take the two variables already chosen as input. The network structure becomes larger.
- (6) When x_i becomes x_j , only the variable sign of this leaf node is changed, and the rest is unchanged. At this time, the network structure is unchanged.

Results

Comparison with symbolic regression algorithms

In order to test the performance of MetaSymNet, we compare the performance of our algorithm with four state-of-the-art symbolic regression algorithms on ten public datasets *Nguyen*, *Keijzer*, *Korns*, *Constant*, *Livermore*, *R*, *Vladislavlev*, *Jin*, *Neat*, *AlFeynman*, and *Others*. Specific formula details are given in Table tables .4 to .8, in the appendix.

- **DSO**, based on DSR, combines DSR and GP algorithm organically.
- **GP**, a classical symbolic regression algorithm based on a genetic algorithm.
- **EQL**, a typical neural network-like symbolic regression algorithm.
- **NeSymReS**, a typical large-scale pre-training algorithm

Fit ability test When doing comparative experiments, we strictly control the experimental variables and ensure that all the other conditions are the same except for the algorithm type to ensure the fairness and credibility of the experiment. Specifically, (1) At test time, on the same test expression, we sample x_i on exactly the same interval for different algorithms. To ensure the consistency of the test data. See Appendix tables .4 to .8, for the specific sampling range of each expression. (2) For some of the "Constraints" used in our algorithm, we also use the exact same "Constraints" in other algorithms. To ensure that the performance of the individual algorithms is not affected by the difference in the "Constraints". In the experiment, we use the coefficient of

determination (R^2)(Nagelkerke et al. 1991; Ozer 1985) to judge how well each algorithm fits the expression. The results are shown in Table 1, from which we see that MetaSymNet achieves the performance of SOTA on multiple datasets. The expression for R^2 is given in the following equation 5:

$$\mathcal{R}^\in = 1 - \frac{\sum_{i=1}^{\mathcal{N}} (y - y_{pred})^2}{\sum_{i=1}^{\mathcal{N}} (y - \bar{y})^2} \quad (5)$$

Where y_{pred} is the predicted y value and \bar{y} is the mean of the true y values.

Anti noise capability test

In the real world, data often contains noise and uncertainty. This noise can come from measurement errors, interference during data acquisition, or other unavoidable sources(Berglund, Hassmen, and Job 1996; Tam et al. 2008; Beall and Lowe 2007). The noise immunity test can simulate the noise situation in the real environment, and help to evaluate the performance of the symbolic regression algorithm in the case of imperfect data, so as to help us understand its reliability and robustness in practical applications. These trials can guide the tuning and selection of the model, ensuring that it will work robustly in real scenarios.(Ziyadinov and Tereshonok 2022; Gao et al. 2020)

We generate noisy data y_{noise} in the following way. To simulate different levels of noise in the real world, we divide the noise into ten levels. First, the noisy data $Data_{noise}$ is obtained by randomly sampling on the interval $[-\mathcal{L} * Span, +\mathcal{L} * Span]$. Here, $\mathcal{L} = [0.00.0.01.0.02, \dots, 0.1]$ is the level of noise. $Span = abs|Max - min(y)(y)|$ is the Span of y . $y_{noise} = y + Data_{noise}$.

We employed the Nguyen dataset to assess the algorithm's resilience to noise perturbations. For each mathematical expression, we conducted 100 iterations at varying noise levels. Subsequently, the R^2 between the curve derived from each individual trial and the original curve was computed, serving as a metric to quantify noise resilience. The final outcome was determined by averaging the results from the 100 trials. The average R^2 values of both MetaSymNet and five prominent strong symbolic regression baselines were compared across different noise levels, and the results are depicted in Figure 3a. Notably, the comprehensive analysis demonstrates that MetaSymNet exhibits superior anti-noise performance in contrast to the other four strong symbolic regression baselines.

Comparison with traditional machine learning algorithms

In order to test the comprehensive performance of MetaSymNet compared with traditional neural Network (MLP)(Rumelhart, Hinton, and Williams 1986) and Support Vector Machine (SVM)(Drucker et al. 1996). We conduct a series of test experiments on the performance of MetaSymNet, MPL, and SVM on the Nguyen dataset. The experiments mainly include the test of fitting ability, extrapolation test, and network structure complexity test.

Fit ability test As the name suggests, this test tests how well three algorithms fit the data. In the test, we sample x_i

Benchmark	Expression	MetaSymNet		MLP		SVR	
		Inside	Outside	Inside	Outside	Inside	Outside
Nguyen-1	$x^3 + x^2 + x$	1.0	1.0	0.9999	-32.47	0.9999	-59.33
Nguyen-2	$x^4 + x^3 + x^2 + x$	1.0	1.0	0.9999	-121.36	0.9998	-425.28
Nguyen-3	$x^5 + x^4 + x^3 + x^2 + x$	0.9999	0.9725	0.9999	-602.86	0.9942	-410.12
Nguyen-4	$x^6 + x^5 + x^4 + x^3 + x^2 + x$	0.9999	0.9382	0.9982	-3002.18	0.9847	-4908.16
Nguyen-5	$\sin(x^2) \cos(x) - 1$	0.9999	0.2344	0.9916	-12.46	0.5322	-27.36
Nguyen-6	$\sin(x) + \sin(x + x^2)$	1.0	1.0	0.9992	-10.15	0.9918	-3.34
Nguyen-7	$\log(x + 1) + \log(x^2 + 1)$	0.9938	0.9462	0.9999	0.56	0.9817	-60.15
Nguyen-8	\sqrt{x}	1.0	1.0	0.9998	0.69	0.9493	-48.42
Nguyen-9	$\sin(x) + \sin(y^2)$	1.0	1.0	0.9999	-2.21	0.9444	-52.39
Nguyen-10	$2 \sin(x) \cos(y)$	1.0	1.0	0.9949	-18.56	0.9863	-2.95
Nguyen-11	x^y	0.9999	0.9921	0.9999	-137892	0.9924	-901002
Nguyen-12	$x^4 - x^3 + \frac{1}{2}y^2 - y$	0.9972	-1.818	0.9928	-610.21	0.9904	-7822.80
	Average	0.9999	0.6888	0.9980	-11858.60	0.9456	-76235.19

Table 2: Comparison of extrapolation and R^2 between MetaSymNet, MLP, and SVR. .

Benchmark	MetaSymNet		MLP	
	Nodes	Parameters	Nodes	Parameters
Nguyen-1	5	22	15	70
Nguyen-2	9	38	17	94
Nguyen-3	14	58	18	106
Nguyen-4	20	82	25	185
Nguyen-5	5	16	25	185
Nguyen-6	5	18	8	22
Nguyen-7	4	16	12	34
Nguyen-8	1	4	16	82
Nguyen-9	3	10	40	360
Nguyen-10	4	14	130	3190
Nguyen-11	3	6	16	88
Nguyen-12	10	40	16	96
Average	6.75	27	28.16	376

Table 3: Comparison of the number of nodes and parameters used by MetaSymNet and MLP when the R^2 is greater than 0.99.

on the interval $[-2,2]$, and then use three algorithms to fit the same data points, using R^2 as the evaluation metric. The experimental results are shown in Table 2, from which it can be seen that MetaSymNet slightly outperforms MLP and SVR in terms of fitting ability.

Test for extrapolation Extrapolation is the ability to test how well the trained model of the algorithm fits outside of the training data. Let’s say we sample the variable x in the interval $[-2, 2]$ and use this data to train a neural network. If the trained model can fit the data well in the interval, will it perform as well in the interval $[-5,5]$ as in the interval $[-2,2]$ To do this, we sample x on the interval $[-2,2]$ and train MetaSymNet, MLP, and SVR on the sampled data. Then the models trained by the above three algorithms are tested on the intervals $[-2,2]$ and $[-5,5]$, respectively. Table 2 shows the performance of MetaSymNet, MLP as well as SVR. We can see that MetaSymNet and both baselines perform well in the range $[-2,2]$ (Insaid). However, when we expand the range

to $[-5,5]$ (Outsaid), MetaSymNet still performs well, while MLP and SVR perform less well. Because the activation functions of MetaSymNet are more diverse, the network has a stronger representation ability. Therefore, compared with MLP, it is easier to obtain results with stronger extrapolation. The picture of the extrapolation effect is shown in Figure 3b

Network structure complexity test The network structure of the traditional neural network is fixed, and it can not adjust network structure dynamically according to the complexity of the problem. It is easy to cause the phenomenon of redundant network structure and parameters. MetaSymNet’s network structure is dynamically adjusted according to the complexity of the problem, which can greatly improve the network structure and parameter redundancy. In order to test the structural optimization ability of MetaSymNet, we compare the structural complexity of MLP using an iterative pruning strategy(Castellano, Fanelli, and Pelillo 1997) and MetaSymNet on the Nguyen dataset. Specifically, we compare the number of neurons and parameters used by the two algorithms when R^2 reaches 0.99. The detailed statistical results are shown in Table 3. As can be seen from the table, MetaSymNet has a simpler architecture and a smaller number of parameters at the same level of R^2 . And the more complex the problem, the more obvious this advantage will be.

Discussion

In this paper, we introduce a novel neural network architecture, named MetaSymNet. The algorithm has achieved good results in fitting ability, anti-noise ability, and extrapolation ability. Unlike previous neural networks, MetaSymNet’s architecture is not static but dynamically adjusted during the training process according to the requirements of the problem. The network size can be freely adjusted according to the need, which can be expanded or reduced to meet the requirements of specific tasks. Experimental results show that MetaSymNet is much smaller than the traditional MLP with the same accuracy. This makes our model more lightweight and easier to deploy on the hardware side. Especially in areas sensitive to response speed, such as face locks(Shanthi, Sivalak-

shmi et al. 2023), face unlocking mobile phones(Sivalenka et al. 2022), and autonomous driving(Zhang et al. 2022), this feature has a significant advantage. In this paper, we propose a novel activation function called PANGU meta-function. The function can autonomously evolve into $[+, -, \times, \div, \sin, \cos, \sqrt{}, \exp, \log]$ and other basic functions under the control of internal selection parameters, which greatly improves the representation ability of neural networks. This also makes the final result of MetSymNet a concise, interpretable mathematical expression. The interpretability and analyzability of the results make our algorithm more credible. This makes our algorithm a very broad application in some fields involving high-risk decisions, such as finance, medicine, and law. Because these are domains where decisions can have a significant impact on people’s lives, people need to be able to understand and trust the decision-making process of the algorithm.

Despite the satisfactory results obtained by our algorithm, there are still some shortcomings. For example, some hyperparameters, such as the regulation coefficient λ in the loss function that controls the proportion of entropy loss, are difficult to tune. Moreover, the method occasionally gets stuck in local optima, and for some expressions, it is difficult to find the original expression and only approximate results can be obtained. In the future, we will consider changing the way PANGU metafunctions evolve. In the activation function selection, we will not use the greedy selection strategy, but a series of other search methods such as beam search, Monte Carlo tree search, etc., to significantly improve the search efficiency and performance of the algorithm.

References

- Abd Elaziz, M.; Dahou, A.; Abualigah, L.; Yu, L.; Alshinwan, M.; Khasawneh, A. M.; and Lu, S. 2021. Advanced metaheuristic optimization techniques in applications of deep neural networks: a review. *Neural Computing and Applications*, 1–21.
- Afnan, M. A. M.; Liu, Y.; Conitzer, V.; Rudin, C.; Mishra, A.; Savulescu, J.; and Afnan, M. 2021. Interpretable, not black-box, artificial intelligence should be used for embryo selection.
- Augusto, D. A.; and Barbosa, H. J. 2000. Symbolic regression via genetic programming. In *Proceedings. Vol. 1. Sixth Brazilian symposium on neural networks*, 173–178. IEEE.
- Beall, E. B.; and Lowe, M. J. 2007. Isolating physiologic noise sources with independently determined spatial measures. *Neuroimage*, 37(4): 1286–1300.
- Berglund, B.; Hassmen, P.; and Job, R. S. 1996. Sources and effects of low-frequency noise. *The Journal of the Acoustical Society of America*, 99(5): 2985–3002.
- Biggio, L.; Bendinelli, T.; Neitz, A.; Lucchi, A.; and Parascandolo, G. 2021. Neural symbolic regression that scales. In *International Conference on Machine Learning*, 936–945. PMLR.
- Bottou, L. 2010. Large-scale machine learning with stochastic gradient descent. In *Proceedings of COMPSTAT’2010: 19th International Conference on Computational Statistics Paris France, August 22-27, 2010 Keynote, Invited and Contributed Papers*, 177–186. Springer.
- Bottou, L. 2012. Stochastic gradient descent tricks. In *Neural Networks: Tricks of the Trade: Second Edition*, 421–436. Springer.
- Castellano, G.; Fanelli, A. M.; and Pelillo, M. 1997. An iterative pruning algorithm for feedforward neural networks. *IEEE transactions on Neural networks*, 8(3): 519–531.
- Cheng, Y.; Yu, F. X.; Feris, R. S.; Kumar, S.; Choudhary, A.; and Chang, S.-F. 2015. An exploration of parameter redundancy in deep networks with circulant projections. In *Proceedings of the IEEE international conference on computer vision*, 2857–2865.
- Dai, Y.-H. 2002. Convergence properties of the BFGS algorithm. *SIAM Journal on Optimization*, 13(3): 693–701.
- Dong, X.; Zhu, X.; and Ma, D. 2019. Hardware implementation of softmax function based on piecewise LUT. In *2019 IEEE International Workshop on Future Computing (IWOFc)*, 1–3. IEEE.
- Drucker, H.; Burges, C. J.; Kaufman, L.; Smola, A.; and Vapnik, V. 1996. Support vector regression machines. *Advances in neural information processing systems*, 9.
- Espejo, P. G.; Ventura, S.; and Herrera, F. 2009. A survey on the application of genetic programming to classification. *IEEE Transactions on Systems, Man, and Cybernetics, Part C (Applications and Reviews)*, 40(2): 121–144.
- Esterhuizen, J. A.; Goldsmith, B. R.; and Linic, S. 2022. Interpretable machine learning for knowledge generation in heterogeneous catalysis. *Nature Catalysis*, 5(3): 175–184.
- Fortin, F.-A.; De Rainville, F.-M.; Gardner, M.-A. G.; Parizeau, M.; and Gagné, C. 2012. DEAP: Evolutionary algorithms made easy. *The Journal of Machine Learning Research*, 13(1): 2171–2175.
- Gao, X.; Saha, R. K.; Prasad, M. R.; and Roychoudhury, A. 2020. Fuzz testing based data augmentation to improve robustness of deep neural networks. In *Proceedings of the acm/ieee 42nd international conference on software engineering*, 1147–1158.
- Guidotti, R.; Monreale, A.; Ruggieri, S.; Turini, F.; Giannotti, F.; and Pedreschi, D. 2018. A survey of methods for explaining black box models. *ACM computing surveys (CSUR)*, 51(5): 1–42.
- Hermundstad, A. M.; Brown, K. S.; Bassett, D. S.; and Carlson, J. M. 2011. Learning, memory, and the role of neural network architecture. *PLoS computational biology*, 7(6): e1002063.
- Kamienny, P.-A.; d’Ascoli, S.; Lample, G.; and Charton, F. 2022. End-to-end symbolic regression with transformers. *Advances in Neural Information Processing Systems*, 35: 10269–10281.
- Katoch, S.; Chauhan, S. S.; and Kumar, V. 2021. A review on genetic algorithm: past, present, and future. *Multimedia tools and applications*, 80: 8091–8126.

- Kim, S.; Lu, P. Y.; Mukherjee, S.; Gilbert, M.; Jing, L.; Čeperić, V.; and Soljačić, M. 2020. Integration of neural network-based symbolic regression in deep learning for scientific discovery. *IEEE transactions on neural networks and learning systems*, 32(9): 4166–4177.
- Liu, D. C.; and Nocedal, J. 1989. On the limited memory BFGS method for large scale optimization. *Mathematical programming*, 45(1-3): 503–528.
- Liu, W.; Wang, Z.; Liu, X.; Zeng, N.; Liu, Y.; and Alsaadi, F. E. 2017. A survey of deep neural network architectures and their applications. *Neurocomputing*, 234: 11–26.
- Maksimenko, V. A.; Kurkin, S. A.; Pitsik, E. N.; Musatov, V. Y.; Runnova, A. E.; Efremova, T. Y.; Hramov, A. E.; and Pisarchik, A. N. 2018. Artificial neural network classification of motor-related eeg: An increase in classification accuracy by reducing signal complexity. *Complexity*, 2018.
- Mamoshina, P.; Vieira, A.; Putin, E.; and Zhavoronkov, A. 2016. Applications of deep learning in biomedicine. *Molecular pharmaceutics*, 13(5): 1445–1454.
- Marcinkevičs, R.; and Vogt, J. E. 2020. Interpretability and explainability: A machine learning zoo mini-tour. *arXiv preprint arXiv:2012.01805*.
- Martius, G.; and Lampert, C. H. 2016. Extrapolation and learning equations. *arXiv preprint arXiv:1610.02995*.
- Mirjalili, S.; and Mirjalili, S. 2019. Genetic algorithm. *Evolutionary Algorithms and Neural Networks: Theory and Applications*, 43–55.
- Mundhenk, T. N.; Landajuela, M.; Glatt, R.; Santiago, C. P.; Faissol, D. M.; and Petersen, B. K. 2021. Symbolic regression via neural-guided genetic programming population seeding. *arXiv preprint arXiv:2111.00053*.
- Nagelkerke, N. J.; et al. 1991. A note on a general definition of the coefficient of determination. *biometrika*, 78(3): 691–692.
- Narayanan, H.; Bournazou, M. N. C.; Gosálbez, G. G.; and Butté, A. 2022. Functional-Hybrid modeling through automated adaptive symbolic regression for interpretable mathematical expressions. *Chemical Engineering Journal*, 430: 133032.
- Ozer, D. J. 1985. Correlation and the coefficient of determination. *Psychological bulletin*, 97(2): 307.
- Petersen, B. K.; Landajuela, M.; Mundhenk, T. N.; Santiago, C. P.; Kim, S. K.; and Kim, J. T. 2019. Deep symbolic regression: Recovering mathematical expressions from data via risk-seeking policy gradients. *arXiv preprint arXiv:1912.04871*.
- Rényi, A. 1961. On measures of entropy and information. In *Proceedings of the Fourth Berkeley Symposium on Mathematical Statistics and Probability, Volume 1: Contributions to the Theory of Statistics*, volume 4, 547–562. University of California Press.
- Rodríguez, P.; Bautista, M. A.; Gonzalez, J.; and Escalera, S. 2018. Beyond one-hot encoding: Lower dimensional target embedding. *Image and Vision Computing*, 75: 21–31.
- Rumelhart, D. E.; Hinton, G. E.; and Williams, R. J. 1986. Learning representations by back-propagating errors. *nature*, 323(6088): 533–536.
- Shanthi, K.; Sivalakshmi, P.; et al. 2023. Smart drone with real time face recognition. *Materials Today: Proceedings*, 80: 3212–3215.
- Sivalenka, V.; Aluvala, S.; Sneha, Y.; Mannan, K.; Farheen, S.; and Kumaraswamy, E. 2022. An empirical study of various face recognition and face liveness detection techniques and algorithms. In *AIP Conference Proceedings*, volume 2418. AIP Publishing.
- Stevens, J. R.; Venkatesan, R.; Dai, S.; Khailany, B.; and Raghunathan, A. 2021. Softmax: Hardware/software co-design of an efficient softmax for transformers. In *2021 58th ACM/IEEE Design Automation Conference (DAC)*, 469–474. IEEE.
- Sun, F.; Liu, Y.; Wang, J.-X.; and Sun, H. 2022. Symbolic physics learner: Discovering governing equations via monte carlo tree search. *arXiv preprint arXiv:2205.13134*.
- Sun, S.; Chen, W.; Wang, L.; Liu, X.; and Liu, T.-Y. 2016. On the depth of deep neural networks: A theoretical view. In *Proceedings of the AAAI Conference on Artificial Intelligence*, volume 30.
- Tam, C. K.; Viswanathan, K.; Ahuja, K.; and Panda, J. 2008. The sources of jet noise: experimental evidence. *Journal of Fluid Mechanics*, 615: 253–292.
- Udrescu, S.-M.; Tan, A.; Feng, J.; Neto, O.; Wu, T.; and Tegmark, M. 2020. AI Feynman 2.0: Pareto-optimal symbolic regression exploiting graph modularity. *Advances in Neural Information Processing Systems*, 33: 4860–4871.
- Udrescu, S.-M.; and Tegmark, M. 2020. AI Feynman: A physics-inspired method for symbolic regression. *Science Advances*, 6(16): eaay2631.
- Vaswani, A.; Shazeer, N.; Parmar, N.; Uszkoreit, J.; Jones, L.; Gomez, A. N.; Kaiser, Ł.; and Polosukhin, I. 2017. Attention is all you need. *Advances in neural information processing systems*, 30.
- Wehrl, A. 1978. General properties of entropy. *Reviews of Modern Physics*, 50(2): 221.
- Yanco, H. A.; Desai, M.; Drury, J. L.; and Steinfeld, A. 2016. Methods for developing trust models for intelligent systems. *Robust intelligence and trust in autonomous systems*, 219–254.
- Zhang, X.; Du, B.; Wu, Z.; and Wan, T. 2022. LAANet: lightweight attention-guided asymmetric network for real-time semantic segmentation. *Neural Computing and Applications*, 34(5): 3573–3587.
- Ziyadinov, V.; and Tereshonok, M. 2022. Noise immunity and robustness study of image recognition using a convolutional neural network. *Sensors*, 22(3): 1241.

Appendix: Pseudocode for the MetSymNet

Algorithm 1 describes the overall process of MetSymNet in detail. We first initialize a tree-like network structure, where the neurons of the internal nodes of the network are PANGU metafunctions and the neurons of the leaf nodes are variable metafunctions. We first iterate N_{DB} times to optimize the amplitude parameter D and bias parameter B of each node. We then iterate N_{ZW} times to optimize the selection parameters \mathbb{Z}, \mathbb{W} . We then use **ExtractingExpression**($\mathbb{Z}, \mathbb{W}, D, B$) to evolve the neuron into a basic function, resulting in a concise expression. Then we can further optimize the parameters in the expression. Repeat the above process until r^2 reaches the desired value,

Algorithm 1: MetaSymNet

Data: $X = [x_1, x_2, \dots, x_m]$; $y = [y_1, y_2, \dots, y_m]$; $S = [s_1, s_2, \dots, s_n]$;
 $D = [d_1, d_2, \dots, d_n]$; $B = [b_1, b_2, \dots, b_n]$;
 $\mathbb{Z} = [Z_1, Z_2, \dots, Z_n]$; $\mathbb{W} = [W_1, W_2, \dots, W_n]$.

Result: Find an expression such that $y = f(X)$

- 1 **Initialize the network structure**
- 2 **while** $R^2 \leq 0.9999$ **do**
 - 3 \triangleright A threshold can also be set, for example, $R^2 \geq 0.9999$.
 - 4 **repeat**
 - 5 **for** $j \leftarrow 1$ **to** N_{DB} **do**
 - 6 **NumericalOptimization** (D, B) \triangleright N_{DB} denotes the number of optimization rounds for the parameters D and B
 - 7 **end**
 - 8 **for** $j \leftarrow 1$ **to** N_{ZW} **do**
 - 9 **NumericalOptimization** (\mathbb{Z}, \mathbb{W}) \triangleright Optimizing the internal selection parameters \mathbb{Z}, \mathbb{W} of PANGU metafunction and variable metafunction.
 - 10 **end**
 - 11 **ExtractingExpression**($\mathbb{Z}, \mathbb{W}, D, B$) \triangleright Based on the optimized selected parameters, a concise mathematical expression is extracted from the network.
 - 12 **ConstantRefine**(d, b) \triangleright Taking the extracted $[d, b]$ as the initial value, the constants are further optimized by the numerical optimization algorithm.
 - 13 **Obtaining the formula** : $y_{pred} = F(x_1, x_2, \dots, x_n)$
 - 14 **Calculate** R^2
 - 15 **if** $R^2 > T$ **then**
 - 16 \triangleright T represents the termination threshold of the algorithm
 - 17 **break**; \triangleright Terminate the program upon achieving expected R^2
 - 18 **end**
 - 19 **until** *Reach predetermined accuracy*;
 - 20 **end**

Algorithm 2 This pseudocode describes in detail the evolution process of PANGU meta-functions and Variable meta-functions in MetSymNet to basic functions and variables. For the PANGU meta-function, we first choose the index I corresponding to the maximum value in its function selection parameter Z . Then the corresponding symbol s is selected according to the index I . The principle of Variable meta-functions is similar to PANGU meta-functions, except that the target is a variable of type $[x_1, x_2, \dots, x_m]$.

Algorithm 2: ExtractingExpression($\mathbb{Z}, \mathbb{W}, D, B$)

```
1 Input :  $D = [d_1, d_2, \dots, d_n]; B = [b_1, b_2, \dots, b_n];$   
2  $\mathbb{Z} = [Z_1, Z_2, \dots, Z_n]; \mathbb{W} = [W_1, W_2, \dots, W_n]$   
3 Output :  $Aexpression : F = (x_1, \dots, x_m)$   
4  $S \leftarrow [s_1, s_2, \dots, s_n]$   
5  $Symbol \leftarrow [+ , - , \times , \div , sin , \dots , x_1 , \dots , x_m]$  ▷ Activation function library.  
6  $X \leftarrow [x_1, x_1, \dots, x_m]$  ▷ Candidate variables.  
7 for  $s \leftarrow S$  do  
8   if  $sisPANGU\_metafunction$  then  
9      $\mathbf{I} \leftarrow Max\_index(Z_s)$  ▷ The activation function is selected according to the activation function selection  
     parameter  $Z$   
10     $s \leftarrow Symbol[I]$   
11  end  
12  if  $sisVariable\_metafunction$  then  
13     $\mathbf{I} \leftarrow Max\_index(W_s)$  ▷ The variable type is selected according to the variable selection parameter  $W$ .  
14     $s \leftarrow X[I]$   
15  end  
16 end
```

Appendix: Backpropagation derivation (Use SGD)

Forward propagation :

$$\begin{aligned} OUT_1 &= [\sin(x), \cos(x), \dots, \exp(x)] * \left[\frac{e^{z_{11}}}{\sum_{i=1}^n e^{z_{1i}}}, \frac{e^{z_{12}}}{\sum_{i=1}^n e^{z_{1i}}}, \dots, \frac{e^{z_{1n}}}{\sum_{i=1}^n e^{z_{1i}}} \right] \\ &= \sin(x) * e_{11} + \cos(x) * e_{12} + \dots + \exp(x) * e_{1n} \\ OUT_2 &= [\sin(OUT_1), \cos(OUT_1), \dots, \exp(OUT_1)] * \left[\frac{e^{z_{21}}}{\sum_{i=1}^n e^{z_{2i}}}, \frac{e^{z_{22}}}{\sum_{i=1}^n e^{z_{2i}}}, \dots, \frac{e^{z_{2n}}}{\sum_{i=1}^n e^{z_{2i}}} \right] \\ &= \sin(OUT_1) * e_{21} + \cos(OUT_1) * e_{22} + \dots + \exp(OUT_1) * e_{2n} \\ Loss &= \frac{1}{2} \sum_{i=1}^n (Y_i - OUT_{2i})^2 \end{aligned}$$

Back propagation :

$$\begin{aligned} \frac{\partial Loss}{\partial OUT_2} &= OUT_2 - Y \\ \frac{\partial Loss}{\partial z_{2i}} &= \frac{\partial Loss}{\partial OUT_2} * \frac{\partial OUT_2}{\partial z_{2i}} \\ &= - \frac{\partial Loss}{\partial OUT_2} * [\sin(OUT_1), \cos(OUT_1), \dots, \exp(OUT_1)] * e_{2i}(e_{21}, \dots, e_{2i} - 1, \dots, e_{2n}) \\ &= (OUT_2 - Y) * [\sin(OUT_1), \cos(OUT_1), \dots, \exp(OUT_1)] * e_{2i}(e_{21}, \dots, e_{2i} - 1, \dots, e_{2n}) \\ \frac{\partial Loss}{\partial OUT_1} &= \frac{\partial Loss}{\partial OUT_2} * \frac{\partial OUT_2}{\partial OUT_1} \\ &= (OUT_2 - Y) * (\cos(OUT_1) * e_{21} - \sin(OUT_1) * e_{22} + \dots + \exp(OUT_1) * e_{2n}) \\ \frac{\partial Loss}{\partial z_{1i}} &= \frac{\partial Loss}{\partial OUT_2} * \frac{\partial OUT_2}{\partial OUT_1} * \frac{\partial OUT_1}{\partial z_{1i}} \\ &= - \frac{\partial Loss}{\partial OUT_2} * \frac{\partial OUT_2}{\partial OUT_1} * [\sin(x), \cos(x), \dots, \exp(x)] * e_{1i}(e_{11}, \dots, e_{1i} - 1, \dots, e_{1n}) \end{aligned}$$

Parameter updates

$$\begin{aligned} z_{2i} &= z_{2i} - \alpha \frac{\partial Loss}{\partial z_{2i}} \\ z_{1i} &= z_{1i} - \alpha \frac{\partial Loss}{\partial z_{1i}} \end{aligned}$$

Appendix: Test data in detail

Table tables .4 to .6 shows in detail the expression forms of the data set used in the experiment, as well as the sampling range and sampling number. Some specific presentation rules are described below

- The variables contained in the regression task are represented as $[x_1, x_2, \dots, x_n]$.
- $U(a, b, c)$ signifies c random points uniformly sampled between a and b for each input variable. Different random seeds are used for training and testing datasets.
- $E(a, b, c)$ indicates c points evenly spaced between a and b for each input variable.

Name	Expression	Dataset
Nguyen-1	$x_1^3 + x_1^2 + x_1$	U(-1, 1, 20)
Nguyen-2	$x_1^4 + x_1^3 + x_1^2 + x_1$	U(-1, 1, 20)
Nguyen-3	$x_1^5 + x_1^4 + x_1^3 + x_1^2 + x_1$	U(-1, 1, 20)
Nguyen-4	$x_1^6 + x_1^5 + x_1^4 + x_1^3 + x_1^2 + x_1$	U(-1, 1, 20)
Nguyen-5	$\sin(x_1^2) \cos(x) - 1$	U(-1, 1, 20)
Nguyen-6	$\sin(x_1) + \sin(x_1 + x_1^2)$	U(-1, 1, 20)
Nguyen-7	$\log(x_1 + 1) + \log(x_1^2 + 1)$	U(0, 2, 20)
Nguyen-8	\sqrt{x}	U(0, 4, 20)
Nguyen-9	$\sin(x) + \sin(x_2^2)$	U(0, 1, 20)
Nguyen-10	$2 \sin(x) \cos(x_2)$	U(0, 1, 20)
Nguyen-11	$x_1^{x_2}$	U(0, 1, 20)
Nguyen-12	$x_1^4 - x_1^3 + \frac{1}{2}x_2^2 - x_2$	U(0, 1, 20)
Nguyen-2'	$4x_1^4 + 3x_1^3 + 2x_1^2 + x$	U(-1, 1, 20)
Nguyen-5'	$\sin(x_1^2) \cos(x) - 2$	U(-1, 1, 20)
Nguyen-8'	$\sqrt[3]{x}$	U(0, 4, 20)
Nguyen-8''	$\sqrt[3]{x_1^2}$	U(0, 4, 20)
Nguyen-1 ^c	$3.39x_1^3 + 2.12x_1^2 + 1.78x$	U(-1, 1, 20)
Nguyen-5 ^c	$\sin(x_1^2) \cos(x) - 0.75$	U(-1, 1, 20)
Nguyen-7 ^c	$\log(x + 1.4) + \log(x_1^2 + 1.3)$	U(0, 2, 20)
Nguyen-8 ^c	$\sqrt{1.23x}$	U(0, 4, 20)
Nguyen-10 ^c	$\sin(1.5x) \cos(0.5x_2)$	U(0, 1, 20)
Korns-1	$1.57 + 24.3 * x_1^4$	U(-1, 1, 20)
Korns-2	$0.23 + 14.2 \frac{(x_4 + x_1)}{(3x_2)}$	U(-1, 1, 20)
Korns-3	$4.9 \frac{(x_2 - x_1 + \frac{x_1}{3})}{(3x_3)} - 5.41$	U(-1, 1, 20)
Korns-4	$0.13 \sin(x_1) - 2.3$	U(-1, 1, 20)
Korns-5	$3 + 2.13 \log(x_5)$	U(-1, 1, 20)
Korns-6	$1.3 + 0.13 \sqrt{ x_1 }$	U(-1, 1, 20)
Korns-7	$2.1(1 - e^{-0.55x_1})$	U(-1, 1, 20)
Korns-8	$6.87 + 11 \sqrt{ 7.23x_1x_4x_5 }$	U(-1, 1, 20)
Korns-9	$12 \sqrt{ 4.2x_1x_2x_2 }$	U(-1, 1, 20)
Korns-10	$0.81 + 24.3 \frac{2x_1 + 3x_2^2}{4x_3^3 + 5x_4^4}$	U(-1, 1, 20)
Korns-11	$6.87 + 11 \cos(7.23x_1^3)$	U(-1, 1, 20)
Korns-12	$2 - 2.1 \cos(9.8x_1^3) \sin(1.3x_5)$	U(-1, 1, 20)
Korns-13	$32.0 - 3.0 \frac{\tan(x_1) \tan(x_3)}{\tan(x_2) \tan(x_4)}$	U(-1, 1, 20)
Korns-14	$22.0 - (4.2 \cos(x_1) - \tan(x_2)) \frac{\tanh(x_3)}{\sin(x_4)}$	U(-1, 1, 20)
Korns-15	$12.0 - \frac{6.0 \tan(x_1)}{e^{x_2}} (\log(x_3) - \tan(x_4))$	U(-1, 1, 20)
Jin-1	$2.5x_1^4 - 1.3x_1^3 + 0.5x_2^2 - 1.7x_2$	U(-3, 3, 100)
Jin-2	$8.0x_1^2 + 8.0x_2^3 - 15.0$	U(-3, 3, 100)
Jin-3	$0.2x_1^3 + 0.5x_2^3 - 1.2x_2 - 0.5x_1$	U(-3, 3, 100)
Jin-4	$1.5 \exp x + 5.0 \cos(x_2)$	U(-3, 3, 100)
Jin-5	$6.0 \sin(x_1) \cos(x_2)$	U(-3, 3, 100)
Jin-6	$1.35x_1x_2 + 5.5 \sin((x_1 - 1.0)(x_2 - 1.0))$	U(-3, 3, 100)

Table .4: Specific formula form and value range of the three data sets Nguyen, Korns, and Jin.

Name	Expression	Dataset
Neat-1	$x_1^4 + x_1^3 + x_1^2 + x$	U(-1, 1, 20)
Neat-2	$x_1^5 + x_1^4 + x_1^3 + x_1^2 + x$	U(-1, 1, 20)
Neat-3	$\sin(x_1^2) \cos(x) - 1$	U(-1, 1, 20)
Neat-4	$\log(x + 1) + \log(x_1^2 + 1)$	U(0, 2, 20)
Neat-5	$2 \sin(x) \cos(x_2)$	U(-1, 1, 100)
Neat-6	$\sum_{k=1}^x \frac{1}{k}$	E(1, 50, 50)
Neat-7	$2 - 2.1 \cos(9.8x_1) \sin(1.3x_2)$	E(-50, 50, 10 ⁵)
Neat-8	$\frac{e^{-(x_1)^2}}{1.2+(x_2-2.5)^2}$	U(0.3, 4, 100)
Neat-9	$\frac{1}{1+x_1^{-4}} + \frac{1}{1+x_2^{-4}}$	E(-5, 5, 21)
Keijzer-1	$0.3x_1 \sin(2\pi x_1)$	U(-1, 1, 20)
Keijzer-2	$2.0x_1 \sin(0.5\pi x_1)$	U(-1, 1, 20)
Keijzer-3	$0.92x_1 \sin(2.41\pi x_1)$	U(-1, 1, 20)
Keijzer-4	$x_1^3 e^{-x_1} \cos(x_1) \sin(x_1) \sin(x_1)^2 \cos(x_1) - 1$	U(-1, 1, 20)
Keijzer-5	$3 + 2.13 \log(x_5)$	U(-1, 1, 20)
Keijzer-6	$\frac{x_1(x_1+1)}{2}$	U(-1, 1, 20)
Keijzer-7	$\log(x_1)$	U(0, 1, 20)
Keijzer-8	$\sqrt{(x_1)}$	U(0, 1, 20)
Keijzer-9	$\log(x_1 + \sqrt{x_1^2 + 1})$	U(-1, 1, 20)
Keijzer-10	$\frac{x_1^{x_2}}{x_1^2}$	U(-1, 1, 20)
Keijzer-11	$x_1 x_2 + \sin((x_1 - 1)(x_2 - 1))$	U(-1, 1, 20)
Keijzer-12	$x_1^4 - x_1^3 + \frac{x_2^2}{2} - x_2$	U(-1, 1, 20)
Keijzer-13	$6 \sin(x_1) \cos(x_2)$	U(-1, 1, 20)
Keijzer-14	$\frac{8}{2+x_1^2+x_2^2}$	U(-1, 1, 20)
Keijzer-15	$\frac{x_1^3}{5} + \frac{x_2^3}{2} - x_2 - x_1$	U(-1, 1, 20)
Livermore-1	$\frac{1}{3} + x_1 + \sin(x_1^2)$	U(-3, 3, 100)
Livermore-2	$\sin(x_1^2) * \cos(x_1) - 2$	U(-3, 3, 100)
Livermore-3	$\sin(x_1^3) * \cos(x_1^2) - 1$	U(-3, 3, 100)
Livermore-4	$\log(x_1 + 1) + \log(x_1^2 + 1) + \log(x_1)$	U(-3, 3, 100)
Livermore-5	$x_1^4 - x_1^3 + x_2^2 - x_2$	U(-3, 3, 100)
Livermore-6	$4x_1^4 + 3x_1^3 + 2x_1^2 + x_1$	U(-3, 3, 100)
Livermore-7	$\frac{(exp(x_1) - exp(-x_1))}{2}$	U(-1, 1, 100)
Livermore-8	$\frac{(exp(x_1) + exp(-x_1))}{3}$	U(-3, 3, 100)
Livermore-9	$x_1^9 + x_1^8 + x_1^7 + x_1^6 + x_1^5 + x_1^4 + x_1^3 + x_1^2 + x_1$	U(-1, 1, 100)
Livermore-10	$6 * \sin(x_1) \cos(x_2)$	U(-3, 3, 100)
Livermore-11	$\frac{x_1^2 x_2^2}{(x_1 + x_2)}$	U(-3, 3, 100)
Livermore-12	$\frac{x_1^5}{x_2^4}$	U(-3, 3, 100)
Livermore-13	$x_1^{\frac{3}{2}}$	U(-3, 3, 100)
Livermore-14	$x_1^3 + x_1^2 + x_1 + \sin(x_1) + \sin(x_2^2)$	U(-1, 1, 100)
Livermore-15	$x_1^{\frac{1}{2}}$	U(-3, 3, 100)
Livermore-16	$x_1^{\frac{3}{5}}$	U(-3, 3, 100)
Livermore-17	$4 \sin(x_1) \cos(x_2)$	U(-3, 3, 100)
Livermore-18	$\sin(x_1^2) * \cos(x_1) - 5$	U(-3, 3, 100)
Livermore-19	$x_1^5 + x_1^4 + x_1^2 + x_1$	U(-3, 3, 100)
Livermore-20	$e^{(-x_1^2)}$	U(-3, 3, 100)
Livermore-21	$x_1^8 + x_1^7 + x_1^6 + x_1^5 + x_1^4 + x_1^3 + x_1^2 + x_1$	U(-1, 1, 20)
Livermore-22	$e^{(-0.5x_1^2)}$	U(-3, 3, 100)

Table .5: Specific formula form and value range of the three data sets neat, Keijzer, and Livermore.

Name	Expression	Dataset
Vladislavleva-1	$\frac{e^{-(x_1-1)^2}}{(1.2+(x_2-2.5)^2)}$	U(-1, 1, 20)
Vladislavleva-2	$e^{-x_1} x_1^3 \cos(x_1) \sin(x_1) (\cos(x_1) \sin(x_1)^2 - 1)$	U(-1, 1, 20)
Vladislavleva-3	$e^{-x_1} x_1^3 \cos(x_1) \sin(x_1) (\cos(x_1) \sin(x_1)^2 - 1)(x_2 - 5)$	U(-1, 1, 20)
Vladislavleva-4	$\frac{10}{5+(x_1-3)^2+(x_2-3)^2+(x_3-3)^2+(x_4-3)^2+(x_5-3)^2}$	U(0, 2, 20)
Vladislavleva-5	$30(x_1 - 1) \frac{x_3 - 1}{(x_1 - 10)} x_2^2$	U(-1, 1, 100)
Vladislavleva-6	$6 \sin(x_1) \cos(x_2)$	E(1, 50, 50)
Vladislavleva-7	$2 - 2.1 \cos(9.8x) \sin(1.3x_2)$	E(-50, 50, 10 ⁵)
Vladislavleva-8	$\frac{e^{-(x-1)^2}}{1.2+(x_2-2.5)^2}$	U(0.3, 4, 100)
Test-2	$3.14x_1^2$	U(-1, 1, 20)
Const-Test-1	$5x_1^2$	U(-1, 1, 20)
GrammarVAE-1	$1/3 + x_1 + \sin(x_1^2)$	U(-1, 1, 20)
Sine	$\sin(x_1) + \sin(x_1 + x_1^2)$	U(-1, 1, 20)
Nonic	$x_1^9 + x_1^8 + x_1^7 + x_1^6 + x_1^5 + x_1^4 + x_1^3 + x_1^2 + x_1$	U(-1, 1, 100)
Pagie-1	$\frac{1}{1+x_1^{-4} + \frac{1}{1+x_2^{-4}}}$	E(1, 50, 50)
Meier-3	$\frac{x_1^2 x_2^2}{(x_1+x_2)}$	E(-50, 50, 10 ⁵)
Meier-4	$\frac{x_1^5}{x_2^3}$	U(0.3, 4, 100)
Poly-10	$x_1 x_2 + x_3 x_4 + x_5 x_6 + x_1 x_7 x_9 + x_3 x_6 x_{10}$	E(-1, 1, 100)

Table .6: Specific formula form and value range of the three data sets Vladislavleva and others.

Appendix: MetSymNet tests on AIFeynman dataset.

We evaluated our proposed symbol regression algorithm, MetSymNet, using the AI Feynman dataset, which encompasses problems from physics and mathematics across various subfields like mechanics, thermodynamics, and electromagnetism. While the dataset originally included 100,000 sampled data points, we intentionally limited our analysis to 100 data points to rigorously assess MetSymNet’s performance. Applying MetSymNet to perform symbol regression on each of these data points, we subsequently measured the R^2 values between the predicted outcomes and the correct answers. Our experimental findings clearly demonstrate that MetSymNet adeptly captures the underlying expressions from a limited number of sample points. Remarkably, the R^2 values exceeded 0.99 for the majority of formulas, indicating the algorithm’s proficiency in accurately fitting these expressions. These results firmly establish MetSymNet as a high-performing solution for challenges within the realms of physics and mathematics. The implications are significant, suggesting MetSymNet’s potential for versatile application across various domains. You can find the detailed experimental outcomes in Table .7 and Table .8.

Appendix: Computing resources

The server we employ features an Intel(R) Xeon(R) Gold 5218R CPU, boasting a base frequency of 2.10 GHz. With a generous 20 CPU cores at its disposal, it enables seamless parallel processing, leading to enhanced computational performance. Thanks to its remarkable core count and optimized architecture, the Intel Xeon Gold 5218R proves to be exceptionally well-suited for managing resource-intensive computational tasks and workloads.

Feynman	Equation	R^2
I.6.20a	$f = e^{-\theta^2/2}/\sqrt{2\pi}$	0.9999
I.6.20	$f = e^{-\frac{\theta^2}{2\sigma^2}}/\sqrt{2\pi\sigma^2}$	0.9991
I.6.20b	$f = e^{-\frac{(\theta-\theta_1)^2}{2\sigma^2}}/\sqrt{2\pi\sigma^2}$	0.9881
I.8.14	$d = \sqrt{(x_2 - x_1)^2 + (y_2 - y_1)^2}$	0.9024
I.9.18	$F = \frac{Gm_1m_2}{(x_2-x_1)^2+(y_2-y_1)^2+(z_2-z_1)^2}$	0.9926
I.10.7	$F = \frac{Gm_1m_2}{(x_2-x_1)^2+(y_2-y_1)^2+(z_2-z_1)^2}$	0.9872
I.11.19	$A = x_1y_1 + x_2y_2 + x_3y_3$	0.9999
I.12.1	$F = \mu N_n$	1.0
I.12.2	$F = \frac{q_1q_2}{4\pi\epsilon r^2}$	1.0
I.12.4	$E_f = \frac{q_1}{4\pi\epsilon r^2}$	0.9999
I.12.5	$F = q_2 E_f$	1.0
I.12.11	$F = Q(E_f + Bv \sin \theta)$	0.9999
I.13.4	$K = \frac{1}{2}m(v^2 + u^2 + w^2)$	0.9982
I.13.12	$U = Gm_1m_2(\frac{1}{r_2} - \frac{1}{r_1})$	1.0
I.14.3	$U = mgz$	1.0
I.14.4	$U = \frac{k_{spring}x^2}{2}$	0.9839
I.15.3x	$x_1 = \frac{x-ut}{\sqrt{1-u^2/c^2}}$	0.9793
I.15.3t	$t_1 = \frac{t-ux/c^2}{\sqrt{1-u^2/c^2}}$	0.9638
I.15.10	$p = \frac{m_0v}{\sqrt{1-v^2/c^2}}$	0.9919
I.16.6	$v_1 = \frac{u+v}{1+uv/c^2}$	0.9873
I.18.4	$r = \frac{m_1r_1+m_2r_2}{m_1+m_2}$	0.9794
I.18.12	$\tau = rF \sin \theta$	0.9999
I.18.16	$L = mrv \sin \theta$	0.9999
I.24.6	$E = \frac{1}{4}m(\omega^2 + \omega_0^2)x^2$	0.9986
I.25.13	$V_e = \frac{q}{C}$	1.0
I.26.2	$\theta_1 = \arcsin(n \sin \theta_2)$	0.9999
I.27.6	$f_f = \frac{1}{\frac{1}{d_1} + \frac{1}{d_2}}$	0.9895
I.29.4	$k = \frac{\omega}{c}$	1.0
I.29.16	$x = \sqrt{x_1^2 + x_2^2 - 2x_1x_2 \cos(\theta_1 - \theta_2)}$	0.9828
I.30.3	$I_* = I_{*0} \frac{\sin^2(n\theta/2)}{\sin^2(\theta/2)}$	0.9912
I.30.5	$\theta = \arcsin(\frac{\lambda}{nd})$	0.9822
I.32.5	$P = \frac{q^2a^2}{6\pi\epsilon c^3}$	0.9932
I.32.17	$P = (\frac{1}{2}\epsilon c E_f^2)(8\pi r^2/3)(\omega^4/(\omega^2 - \omega_0^2)^2)$	0.9817
I.34.8	$\omega = \frac{qvB}{p}$	1.0
I.34.10	$\omega = \frac{p}{1-v/c}$	0.9917
I.34.14	$\omega = \frac{1+v/c}{\sqrt{1-v^2/c^2}}\omega_0$	0.9992
I.34.27	$E = \hbar\omega$	0.9999
I.37.4	$I_* = I_1 + I_2 + 2\sqrt{I_1I_2} \cos \delta$	0.9827
I.38.12	$r = \frac{4\pi\epsilon\hbar^2}{mq^2}$	0.9999
I.39.10	$E = \frac{3}{2}p_F V$	0.9999
I.39.11	$E = \frac{1}{\gamma-1}p_F V$	0.9914
I.39.22	$P_F = \frac{nk_b T}{V} - \frac{mgx}{k_b T}$	0.9976
I.40.1	$n = n_0 e^{-\frac{mgx}{k_b T}}$	0.9816
I.41.16	$L_{rad} = \frac{\hbar\omega^3}{\pi^2 c^2 (e^{\frac{\hbar\omega}{k_b T}} - 1)}$	0.9213
I.43.16	$v = \frac{\mu_{drive} q V_e}{d}$	0.9981
I.43.31	$D = \mu_e k_b T$	1.0
I.43.43	$\kappa = \frac{1}{\gamma-1} \frac{k_b v}{A}$	0.9215
I.44.4	$E = nk_b T \ln(\frac{V_2}{V_1})$	0.8017
I.47.23	$c = \sqrt{\frac{\gamma P r}{\rho}}$	0.9733
I.48.20	$E = \frac{mc^2}{\sqrt{1-v^2/c^2}}$	0.8629
I.50.26	$x = x_1[\cos(\omega t) + \alpha \cos(\omega t)^2]$	0.9999

Table .7: Tested Feynman Equations, part 1.

Feynman	Equation	R^2
II.2.42	$P = \kappa(T_2 - T_1)A$	0.8015
II.3.24	$F_E = \frac{P^d}{4\pi r^2}$	0.9813
II.4.23	$V_e = \frac{q}{4\pi\epsilon r}$	0.9972
II.6.11	$V_e = \frac{1}{4\pi\epsilon} \frac{p_d \cos \theta}{r^2}$	0.9883
II.6.15a	$E_f = \frac{3}{4\pi\epsilon} \frac{p_d z}{r^3} \sqrt{x^2 + y^2}$	0.9221
II.6.15b	$E_f = \frac{3}{4\pi\epsilon} \frac{p_d}{r^3} \cos \theta \sin \theta$	0.9917
II.8.7	$E = \frac{3}{5} \frac{q}{4\pi\epsilon d^2}$	0.9816
II.8.31	$E_{den} = \frac{\epsilon E_f^2}{2}$	1.0
II.10.9	$E_f = \frac{\sigma_{den}}{\epsilon} \frac{1}{1+\chi}$	0.9999
II.11.3	$x = \frac{qE_f}{m(\omega_0^2 - \omega^2)}$	0.9824
II.11.7	$n = n_0 \left(1 + \frac{p_d E_f \cos \theta}{k_b T}\right)$	0.8729
II.11.20	$P_* = \frac{n_\rho p_d^2 E_f}{3k_b T}$	0.7225
II.11.27	$P_* = \frac{n\alpha}{1 - n\alpha/3} \epsilon E_f$	0.9817
II.11.28	$\theta = 1 + \frac{n\alpha}{1 - (n\alpha/3)}$	0.9991
II.13.17	$B = \frac{1}{4\pi\epsilon c^2} \frac{2I}{r}$	0.9961
II.13.23	$\rho_c = \frac{\rho_{c0}}{\sqrt{1 - v^2/c^2}}$	0.9622
II.13.34	$j = \frac{\rho_{c0} v}{\sqrt{1 - v^2/c^2}}$	0.9847
II.15.4	$E = -\mu_M B \cos \theta$	0.9999
II.15.5	$E = -p_d E_f \cos \theta$	0.9999
II.21.32	$V_e = \frac{q}{4\pi\epsilon r(1 - v/c)}$	0.9915
II.24.17	$k = \sqrt{\frac{\omega^2}{c^2} - \frac{\pi^2}{d^2}}$	0.9872
II.27.16	$F_E = \epsilon c E_f^2$	0.9917
II.27.18	$E_{den} = \epsilon E_f^2$	0.9993
II.34.2a	$I = \frac{qv}{2\pi r}$	0.9916
II.34.2	$\mu_M = \frac{qvr}{2}$	0.9862
II.34.11	$\omega = \frac{gqB}{2m}$	0.9926
II.34.29a	$\mu_M = \frac{qh}{4\pi m}$	0.9987
II.34.29b	$E = \frac{g\mu_M B J_z}{h}$	0.8219
II.35.18	$n = \frac{n_0}{\exp(\mu_m B/(k_b T)) + \exp(-\mu_m B/(k_b T))}$	0.9512
II.35.21	$M = n_\rho \mu_M \tanh\left(\frac{\mu_M B}{k_b T}\right)$	0.8199
II.36.38	$f = \frac{\mu_m B}{k_b T} + \frac{\mu_m \alpha M}{\epsilon c^2 k_b T}$	0.9250
II.37.1	$E = \mu_M (1 + \chi) B$	0.9999
II.38.3	$F = \frac{YAx}{d}$	0.9999
II.38.14	$\mu_S = \frac{Y}{2(1 + \sigma)}$	0.9999
III.4.32	$n = \frac{1}{e^{\frac{\hbar\omega}{k_b T}} - 1}$	0.9628
III.4.33	$E = \frac{\hbar\omega}{e^{\frac{\hbar\omega}{k_b T}} - 1}$	0.9973
III.7.38	$\omega = \frac{2\mu_M B}{\hbar}$	0.9826
III.8.54	$p_\gamma = \sin\left(\frac{Et}{\hbar}\right)^2$	0.9822
III.9.52	$p_\gamma = \frac{p_d E_f t}{\hbar} \frac{\sin((\omega - \omega_0)t/2)^2}{((\omega - \omega_0)t/2)^2}$	0.7024
III.10.19	$E = \mu_M \sqrt{B_x^2 + B_y^2 + B_z^2}$	0.9948
III.12.43	$L = n\hbar$	0.9924
III.13.18	$v = \frac{2Ed^2 k}{\hbar}$	0.9999
III.14.14	$I = I_0 \left(e^{\frac{qV_e}{k_b T}} - 1\right)$	0.9914
III.15.12	$E = 2U(1 - \cos(kd))$	0.9999
III.15.14	$m = \frac{\hbar^2}{2Ed^2}$	0.9995
III.15.27	$k = \frac{2\pi\alpha}{nd}$	0.9914
III.17.37	$f = \beta(1 + \alpha \cos \theta)$	0.9988
III.19.51	$E = \frac{-mq^4}{2(4\pi\epsilon)^2 \hbar^2} \frac{1}{n^2}$	0.9894
III.21.20	$j = \frac{-\rho_{c0} q A v_{ec}}{m}$	0.7262

Table .8: Tested Feynman Equations, part 2.